

IMPORTANT NOTICE: The current official version of this document is available via the Sandia National Laboratories WIPP Online Documents web site. A printed copy of this document may not be the version currently in effect.

SANDIA NATIONAL LABORATORIES WASTE ISOLATION PILOT PLANT

Analysis Plan for Prediction of the Extent and Permeability of the Disturbed Rock Zone around a WIPP Disposal Room

Task 1.4.1.2

Effective Date: 02/16/07

Authored by:	<u>Byoung Yoon Park</u> Print Name	<u>Original signed by Byoung Yoon Park</u> Signature	<u>2/15/2007</u> Date
Authored by:	<u>Ahmed E. Ismail</u> Print Name	<u>Original signed by Ahmed E. Ismail</u> Signature	<u>2/15/2007</u> Date
Reviewed by:	<u>Courtney G. Herrick</u> Print Name Technical Reviewer	<u>Original signed by Courtney G. Herrick</u> Signature	<u>2/15/2007</u> Date
Reviewed by:	<u>Mario J. Chavez</u> Print Name Quality Assurance Reviewer	<u>Original signed by Angela Guerin for M.J. Chavez</u> Signature	<u>2/15/07</u> Date
Approved by:	<u>Moo Y. Lee</u> Print Name Department Manager	<u>Original signed by Moo Y. Lee</u> Signature	<u>2/15/2007</u> Date

Table of Contents

1	Introduction and Objectives	3
	1.1 Introduction.....	3
	1.2 Objectives	3
2	Approach	4
	2.1 Overview.....	4
	2.2 Extent of the DRZ.....	4
	2.3 Ultrasonic Wave Velocity Test Data	6
	2.4 Solver	10
	2.5 Material Data	10
	2.6 Permeability of the DRZ.....	11
	2.7 Properties of DRZ_2.....	12
	2.8 DRZ and Permeability around the Disposal Room.....	13
3	Software List	13
4	Tasks	14
5	Special Considerations	14
6	Applicable Procedures	15
7	References	15

List of Tables

Table 1. Material properties of WIPP salt used in the analysis.....	10
Table 2. Material properties of anhydrite used in the analysis (Butcher, 1997).....	11
Table 3. Basic properties of DRZ_2 to be specified.....	12
Table 4. Fracture properties of DRZ_2 to be specified	12
Table 5. Codes to be used for the revised DRZ Analysis.....	13

List of Figures

Figure 1. Activity flow diagram for determining the extent and permeability of the DRZ around a WIPP disposal room.....	5
Figure 2. Arrangement and naming scheme for the measurement holes (Holcomb and Hardy, 2001).	8
Figure 3. P-wave velocities (V_p) for all horizontal cross-hole paths arranged in the same order as the physical arrangement of holes in the rib (Holcomb and Hardy, 2001).	9

1 Introduction and Objectives

1.1 Introduction

The Waste Isolation Pilot Plant (WIPP) repository is excavated in a halite layer of the Salado Formation, just above one of the thicker anhydrite layers known as Marker Bed (MB) 139. The stress state is sufficient to promote considerable creep deformation of halite. In addition, fracturing is commonly observed near the excavation surfaces. Compared to other rocks, salt creeps readily in response to differential stresses. Stress-field alteration and creep closure will create a disturbed rock zone (DRZ) around the excavation. Relative to the intact salt, the DRZ exhibits increased porosity (probably as a result of microfracturing) and increased permeability as a result of connecting fractures. Over time, the DRZ properties change as salt creep occurs.

The DRZ has been re-examined in detail since operations initiated because DRZ properties are essential to the design and analysis of the panel closure system. The DRZ is an important feature that is included in the performance assessment (PA) process models used to predict future repository conditions and brine flow to the accessible environment. Furthermore, as modeled, the properties of the DRZ control a significant portion of the brine that can flow into the waste rooms. The three fundamental parameters of the DRZ used in the PA analysis are its extent, its porosity, and its permeability.

The DRZ dimensions and permeability ranges used for the performance assessment verification test (PAVT) were not changed for the recent re-certification performance assessment baseline calculations (PABC) (Leigh et al. 2005). However, field measurements, laboratory observations, numerical modeling, and operational experience show that the extent, porosity, and permeability of the DRZ can be more accurately represented. These properties change with time; in particular, the extent of DRZ decreases as the salt heals. In conjunction with this decrease in the extent of the DRZ, its permeability also decreases, thereby limiting the amount of brine that could flow from the Salado Formation into the disposal rooms.

It is clear that the DRZ will be limited in extent over the regulatory period. Hansen (2003) presents the several avenues of scientific approach that lead to this conclusion. Extensive laboratory salt creep data demonstrate that damage can be assessed in terms of volumetric strain and principal stresses. Stress states that cause dilation are defined in terms of stress invariants, which allow reasonable models of DRZ evolution and devolution (Park and Holland, 2004; Park and Holland, 2006). Permeability measurements performed on WIPP salt show increased permeability with increasing volumetric strain due to creep damage (Stormont, 1990; Pfeifle et al., 1998). In this analysis plan (AP), a procedure to calculate the extent and permeability of the DRZ around the disposal room will be provided. The results of this analysis will be used in BRAGFLO, which simulates the brine and gas flow in and around the repository.

1.2 Objectives

Currently, the DRZ surrounding the WIPP repository is represented by two materials in WIPP PA: DRZ_0, which characterizes the state of the DRZ before closure of the WIPP facility; and DRZ_1, which characterizes the state of the DRZ after closure of the WIPP facility but before the completion of healing in the DRZ. Although it is known that the properties of the DRZ change as the salt heals, there is currently no material present in the parameter database that

takes these changes into account. The objective of this AP is to determine the properties of a new material, to be called DRZ_2, which will better reflect the long-term physical properties of halite of the DRZ after healing has taken place. This material will be used in BRAGFLO to represent the DRZ beyond a certain time to be specified, at which point significant DRZ healing has occurred. The method for calculating the properties of DRZ_2 which are not copied directly from either DRZ_0 or DRZ_1 will be outlined below.

2 Approach

2.1 Overview

The work outlined in this AP follows closely the analysis of the structural response analysis associated with raising the level of the disposal rooms from their original position to the level of Clay Seam G (Park, 2002; Park and Holland 2004; Park and Holland, 2006). The change of DRZ extent with time will be calculated based on the dilatant damage potential. The constant in the dilatancy criterion will be determined by comparing the results of the Room Q access drift analysis with the field data obtained by Holcomb and Hardy (2001). The relationship between the permeability and the volumetric strain of the halite will be defined from the results of a literature survey, while the permeability distribution within the DRZ will be calculated by post-processing the result from Clay Seam G analysis. Figure 1 illustrates the flow diagram for how these calculations feed into determining the DRZ with permeability around the disposal room.

2.2 Extent of the DRZ

The primary task involved in predicting the extent of the DRZ will be a study of the stress responses in the Room Q access drift as a function of time. The methods employed will be the same as those used in the Clay Seam G numerical analysis (Park and Holland, 2004; Park and Holland, 2006) in conjunction with ultrasonic wave velocity field results and fracture density laboratory measurements (Bryan et al., 2002).

Because the layout of the Room Q access drift differs from that of the disposal room as used in the Clay Seam G analysis, it will be necessary to create a new finite element method (FEM) mesh for use in SANTOS, the quasistatic, large-deformation finite element code that was used in the Clay Seam G analysis. The stratigraphy in the vicinity of the Room Q will be constructed from the underground geologic log map in the S90 access to Room Q (Powers, 2000; Domski et al., 1996) and the simplified stratigraphic model used for the disposal room analyses (Stone, 1997a). The dimensions of the access drift will be determined from the S90 as-built survey data (WTS, 1994).

Dilatancy, defined as an increase in volumetric strain under compressive stress (Jaeger and Cook, 1979), is attributed to micro-fracturing or changes in the pore structure of the salt, resulting in an increase in permeability. A dilatant damage criterion is used to delineate potential zones of DRZ in the salt formation. In this analysis, the following dilatancy criterion is used:

$$D = \frac{C \cdot I_1}{\sqrt{J_2}} \quad (1)$$

where D is the damage factor ;
 C is a constant;

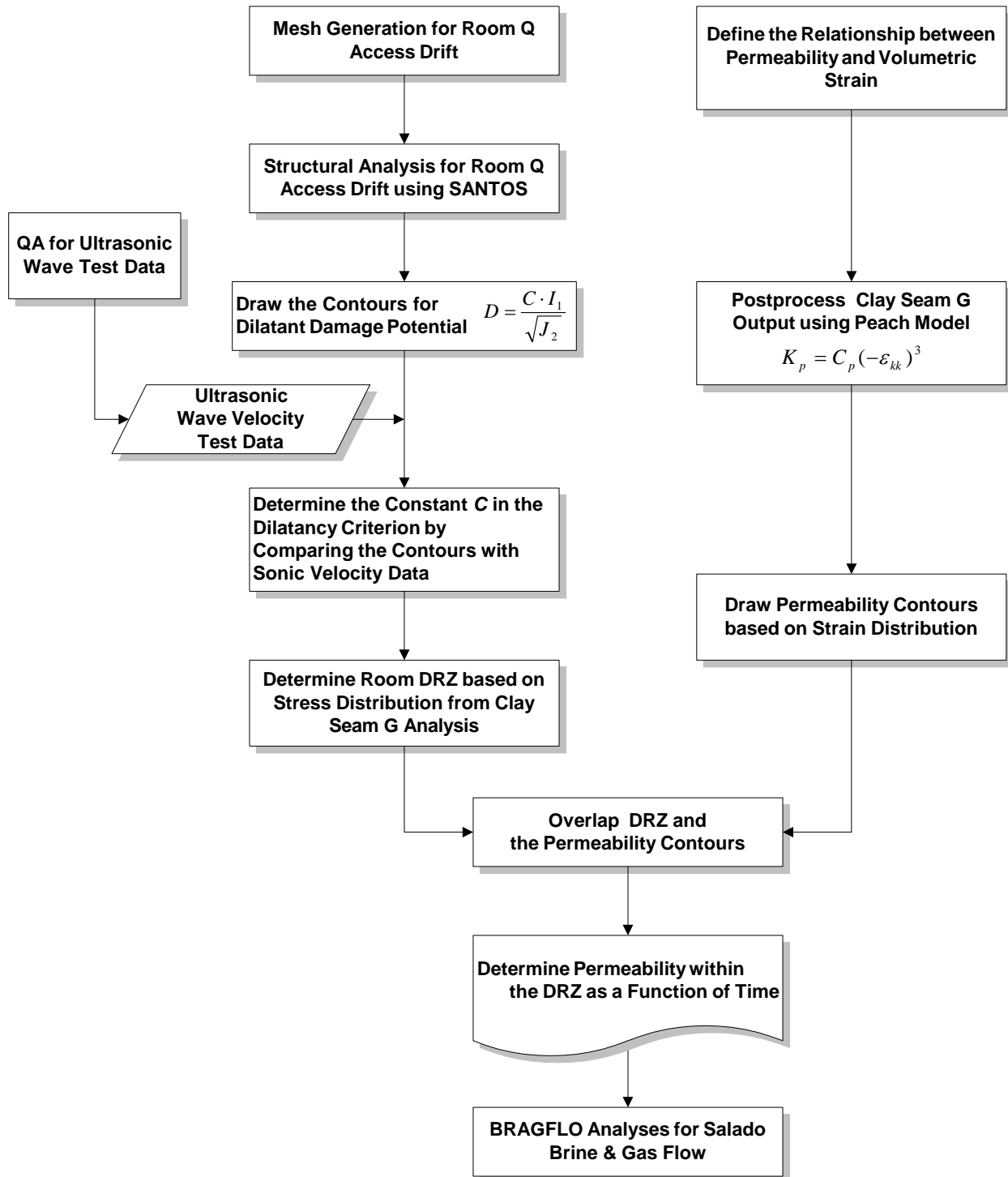


Figure 1. Activity flow diagram for determining the extent and permeability of the DRZ around a WIPP disposal room.

$I_1 = \sigma_1 + \sigma_2 + \sigma_3 = 3\sigma_m$ is the first invariant of the stress tensor;

$J_2 = \frac{(\sigma_1 - \sigma_2)^2 + (\sigma_2 - \sigma_3)^2 + (\sigma_3 - \sigma_1)^2}{6}$ is the second invariant of the deviatoric stress

tensor;

σ_1 , σ_2 , and σ_3 are the maximum, intermediate, and minimum principal stresses; and σ_m is the mean stress.

When $D \leq 1$, the shear stresses in the salt are large relative to the mean stresses, and dilatancy is expected; similarly, when $D > 1$, the shear stresses are small relative to the mean stress, and no dilatancy is expected.

One of our goals is to determine the stresses exerted at the location where the ultrasonic velocity data of Holcomb and Hardy (2001) indicates that the rock in the vicinity of the drift is undamaged. Using the stresses at this location, it will be possible to compute I_1 and J_2 .

As mentioned above, the stresses in the DRZ are expected to change as a function of time. As a result of creep, the volume of the Room Q access drift began to decrease as soon as excavation was completed. Thus, knowledge of the amount of time that lapsed between completion of the excavation and the acquisition of the ultrasonic velocity data is necessary to estimate correctly the value of the parameter C in the damage factor criterion (Eq. 1).

Since there is no waste present in the Room Q access drift, there will be no gas generation to account for in the simulation. Thus, unlike the Clay Seam G analysis, which used a number of values for the gas generation parameter f (Park and Holland, 2004; Park and Holland, 2006), in the proposed analysis, a single simulation with no gas generation, or $f = 0$, will suffice.

Using the results obtained from SANTOS, the quantity C will be determined by computing the two invariants I_1 and J_2 at the location where the ultrasonic velocity data indicates that there is no further damage as a result of excavation. Given the revised value of C , the extent of the DRZ will be assessed by determining the damage factor contours, using the data obtained from the Clay Seam G analysis (Park and Holland, 2004; Park and Holland, 2006).

2.3 Ultrasonic Wave Velocity Test Data

Holcomb and Hardy (2001) performed ultrasonic wave speed measurements to characterize the DRZ in the access drift to Room Q. Measurements were completed at 30 cm (about 1 ft) intervals over paths vertical, horizontal, and perpendicular to the drift axis, giving a complete and redundant data set. Measurements were taken using paths through the salt near the back, floor, and center rib to detect how the varying stress state affects the development of the DRZ in these locations. Figure 2 shows the arrangement and naming scheme for the measurement holes in the access drift to Room Q.

Elastic moduli and, therefore, elastic wave velocities are decreased by open cracks and loosened grain boundaries. The effect on elastic wave velocities is strongest for cracks oriented perpendicular to the particle motion induced by the wave. Thus the physical extent of the disturbed zone can be determined by propagating elastic waves through successive portions of the formation. The undisturbed zone is when the velocity profile remains constant with increasing depth from the rib. In this case, the cracking responsible for the disturbed zone is

expected to vary as a function of distance from the face of the Room Q access drift and to depend on the position of the measurement path relative to the back and floor. Measurements were made between pairs of holes (“cross-hole”) cored perpendicular to the axis of the drift along horizontal and vertical paths lying in vertical planes parallel to the rib. Between each pair of holes, travel time measurements were made at 30 cm intervals to a depth of about 7 meters, as measured from the rib. In addition, measurements were made within one hole (“same-hole”) along paths perpendicular to the drift wall. The paths for the cross-hole measurements were nominally one meter long, while the same-hole measurements all had the same fixed path length of 33 cm. Travel time measurements were made using the technique commonly used for laboratory determinations of sound speed in rock; a sound pulse is applied to the rock at a known time and place and, after traveling through the rock, is received by a transducer at a known distance. P-wave velocity data will be used for “cross-hole”, and P- and S-wave velocity data will be used for “same-hole”. The travel time and distance combine to give the average velocity over that path. Figure 3 shows cross-hole P-wave velocity versus the depth from the rib as an example. DRZ properties determined by fracture analysis are consistent with measured borehole ultrasonic velocity results (Bryan et al., 2002). The petrophysical evidence obtained from laboratory observations of core retrieve from the borehole of QGU14 will be used to verify the ultrasonic data.

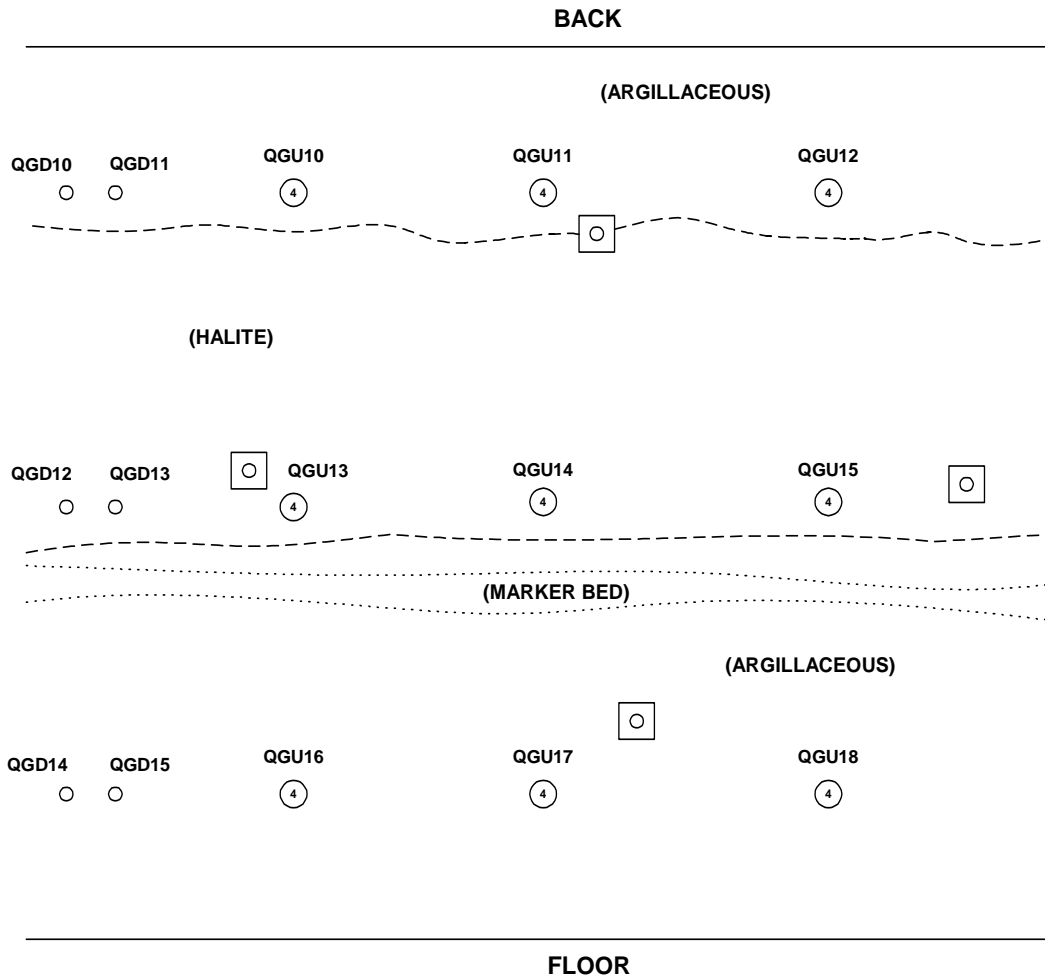
Because of budgetary constraints over the past decade, the ultrasonic wave velocity test was stopped and restarted several times. The erratic work schedule did not allow for the collected data to be reviewed per the quality assurance (QA) program requirements. Thus, the ultrasonic wave velocity tests require that all data calibrations, survey measurements, software routines, and raw data from the ultrasonic wave velocity tests have to be recorded and verified so that they can be used for this analysis (Chavez, 2007a; Chavez 2007b). The MATLAB software routines used for the Holcomb and Hardy (2001) work will be verified as a task for this AP. The other data qualification activities will be handled by the corrective action plan (Chavez, 2007b).

Q ACCESS DRIFT BOREHOLE IDENTIFICATION

LOCATION #1

TERRY MACDONALD & WES DEYONGE
 SANDIA NATIONAL LABORATORIES, DEPT. 6821

DRZ CHAR. TEST PLAN
 03/15/00



BOREHOLE IDENTIFICATION NUMBER:

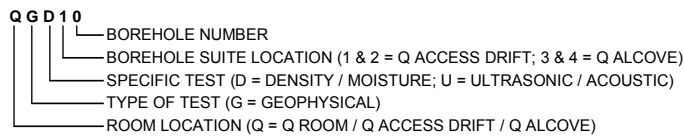


Figure 2. Arrangement and naming scheme for the measurement holes (Holcomb and Hardy, 2001).

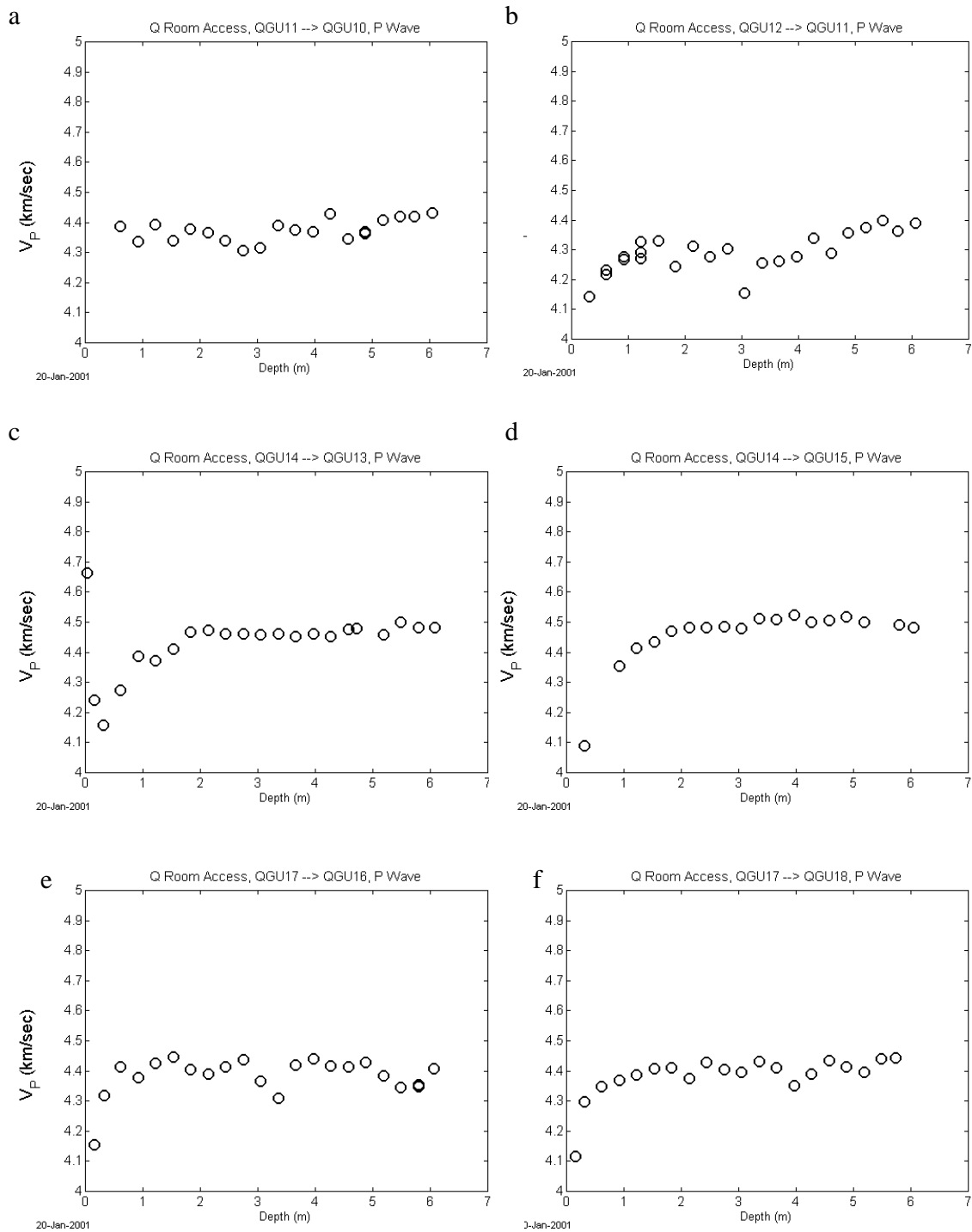


Figure 3. P-wave velocities (V_p) for all horizontal cross-hole paths arranged in the same order as the physical arrangement of holes in the rib (Holcomb and Hardy, 2001).

2.4 Solver

To determine the constant in the dilatancy criterion, the structural analysis for the Room Q access drift will be conducted using the quasistatic, large-deformation finite element code SANTOS. SANTOS is capable of representing 2D planar or axisymmetric geometries. The solution strategy used to obtain the equilibrium states is based on a self-adaptive, dynamic-relaxation solution scheme incorporating proportional damping. The explicit nature of the code means that no stiffness matrix is formed or factorized, thereby reducing the amount of computer storage necessary for execution. The element used in SANTOS is a uniform-strain, 4-node, quadrilateral element with an hourglass control scheme to minimize the effects of spurious deformation modes. Constitutive models for many common engineering materials are available within the code. A robust master-slave contact surfaces algorithm for modeling arbitrary sliding contact is implemented. The executable SANTOS version 2.1.7 is installed on Warthog, a Linux workstation, where it was qualified (WIPP PA, 2003).

The multi-mechanism deformation (M-D) model (Munson and Dawson, 1982; Stone, 1997b) will be used for argillaceous halite and pure halite. The soils and crushable foams model will be used for the anhydrite (Stone, 1997b). Stone (1997a) used the user-supplied subroutine INITST to provide an initial stress state to SANTOS; the unchanged INITST subroutine will be used in this analysis.

2.5 Material Data

The SANTOS data for each material will be identical to that used in Clay Seam G analysis (Park and Holland, 2004). The material constants corresponding to clean and argillaceous salt, which will be used in the analysis, are given in Table 1. The material properties for anhydrite are given in Table 2.

Table 1. Material properties of WIPP salt used in the analysis.

	Parameters		Units	Clean Salt	Argillaceous Salt
Elastic Properties (Butcher, 1997)	Shear modulus	G	MPa	12,400	
	Young's modulus	E	MPa	31,000	
	Poisson's ratio	ν	-	0.25	
Salt Creep Properties (Munson et al., 1989)	Secondary creep constant	A_1	s ⁻¹	8.386×10^{22}	1.407×10^{23}
		B_1		6.086×10^6	8.998×10^6
		A_2		9.672×10^{12}	1.314×10^{13}
		B_2		3.034×10^{-2}	4.289×10^{-2}
	Activation energies	Q_1	cal/mole	25,000	25,000
		Q_2	cal/mole	10,000	10,000
	Stress exponents	n_1	-	5.5	5.5
		n_2		5.0	5.0
	Stress limit of the dislocation slip mechanism	σ_0	MPa	20.57	20.57
	Stress constant	q	-	5,335	5,335
	Transient strain limit constants	M	-	3.0	3.0
		K_0	-	6.275×10^5	2.470×10^6
		c	K ⁻¹	9.198×10^{-3}	9.198×10^{-3}
	Constants for work-hardening parameter	α	-	-17.37	-14.96
		β	-	-7.738	-7.738
Recovery parameter	δ	-	0.58	0.58	

Table 2. Material properties of anhydrite used in the analysis (Butcher, 1997).

Material Property		Units	Anhydrite
Young's modulus		MPa	75,100
Density		kg/m ³	2,300
Poisson's ratio			0.35
Drucker-Prager constants	C	MPa	1.35
	a	-	0.45
Bulk modulus		MPa	83,440
Two mu		MPa	55,630
SANTOS input constants	A ₀	MPa	2.3
	A ₁		2.338

2.6 Permeability of the DRZ

Within the new DRZ, it is necessary to define a new relationship for the permeability as a function of time. Chan and co-workers (Chan et al., 2001) created a model relating permeability both to strain and to networked porosity. The Chan model is a combination of the Carman-Kozeny model of porosity-based permeability (Carman, 1937) and the theoretical work of Peach on the permeability of damaged salt (Peach, 1991). Peach uses percolation theory arguments to define the dilatant strain ε as

$$\varepsilon = \frac{2\pi\langle c \rangle^2 \langle w \rangle \alpha}{\langle l \rangle^3} \quad (2)$$

where $\langle c \rangle$ is the mean crack radius, $\langle w \rangle$ is the mean crack half-width, α is a volumetric shape factor, and $\langle l \rangle$ is the mean crack spacing. The overall expression for the permeability is given by

$$k = \frac{2}{15} \langle w \rangle^2 \varepsilon \alpha p^* \quad (3)$$

where p^* is the fraction of cracks that are part of a connected network. Using the linear relationship between dilatant strain ε and mean crack half-width $\langle w \rangle$, the relationship between permeability and strain can be written as

$$k = \frac{p^* \langle l \rangle^6}{30\pi^2 \alpha \langle c \rangle^4} \varepsilon^3 \quad (4)$$

Rather than attempting to evaluate the prefactors in the above expression, Chan et al. (2001) treats the prefactor as a fitting parameter A to be estimated using experimental data, so that the permeability can be written as

$$k = A \varepsilon^3; \quad (5)$$

however, they do not report the details used to obtain their fitting parameter A. Consequently, we will use the data obtained by Pfeifle et al. (1998) to compute a value for the fitting parameter. With this new parameter value, it will be possible to estimate the permeability in the DRZ as a function of time by using strain values calculated using data from the Clay Seam G analysis (Park and Holland, 2004; Park and Holland, 2006). In particular, the long-term “steady-state” value of the permeability will be used to define a distribution for the parameters DRZ_2:PRMX_LOG, DRZ_2:PRMY_LOG, and DRZ_2:PRMZ_LOG.

2.7 Properties of DRZ_2

In addition to the permeability parameters discussed in the previous section, it will also be necessary to specify the other parameters for DRZ_2. The basic set of parameters which will need to be specified are summarized in Table 3 below. In addition, since the DRZ_2 material may possibly be subject to fracture, it may also be necessary to specify fracture-related properties such as those shown in Table 4.

Table 3. Basic properties of DRZ_2 to be specified (Definitions listed are from the WIPP PAPDB).

Property	Definition	Notes
CAP_MOD	Model number, capillary pressure model	From DRZ_0, DRZ_1, or both
COMP_RCK	Bulk compressibility	From DRZ_0, DRZ_1, or both
KPT	Flag for permeability determined threshold	From DRZ_0, DRZ_1, or both
PC_MAX	Maximum capillary pressure	From DRZ_0, DRZ_1, or both
PCT_A	Threshold pressure constant parameter	From DRZ_0, DRZ_1, or both
PCT_EXP	Threshold pressure exponential parameter	From DRZ_0, DRZ_1, or both
PO_MIN	Minimum brine pressure	From DRZ_0, DRZ_1, or both
PORE_DIS	Pore distribution parameter	From DRZ_0, DRZ_1, or both
POROSITY	Porosity	From DRZ_1
PRMX_LOG	Log of permeability in the x-direction	To be determined from this AP
PRMY_LOG	Log of permeability in the y-direction	To be determined from this AP
PRMZ_LOG	Log of permeability in the z-direction	To be determined from this AP
RELP_MOD	Relative permeability model number	From DRZ_1
SAT_IBRN	Initial brine saturation	From DRZ_0, DRZ_1, or both
SAT_RBRN	Residual brine saturation	From DRZ_0, DRZ_1, or both
SAT_RGAS	Residual gas saturation	From DRZ_0, DRZ_1, or both

Table 4. Fracture properties of DRZ_2 to be specified (Definitions listed are from the WIPP PAPDB).

Property	Definition	Notes
DPHI_MAX	Constant incremental increase in porosity relative to intact salt	To be adapted from S_HALITE
IFRX	Index for fracture permeability enhancement in the x-direction	To be adapted from S_HALITE
IFRY	Index for fracture permeability enhancement in the y-direction	To be adapted from S_HALITE
IFRZ	Index for fracture permeability enhancement in the z-direction	To be adapted from S_HALITE
PF_DELTA	Incremental pressure for full fracture development	To be adapted from S_HALITE
PI_DELTA	Fracture initiation pressure increment	To be adapted from S_HALITE

Most of the property values for DRZ_2 will be taken directly from the corresponding properties of either DRZ_0 or DRZ_1; the exceptions to this are the permeability parameters PRMX_LOG, PRMY_LOG, and PRMZ_LOG, which will be obtained as described above.

2.8 DRZ and Permeability around the Disposal Room

The structural analyses for the Disposal Room were performed to estimate whether raising the repository to Clay Seam G has any significant impact on the conceptual models used in performance assessment (Park and Holland, 2004; Park and Holland, 2006). The calculations used in the Compliance Certification Application (CCA) were replicated and then repeated for grid changes appropriate for the new horizon raised to Clay Seam G. The results of the analyses for both the current room and the raised room will be used for calculating the DRZ with permeability around the disposal rooms.

To calculate the DRZ extent at specific times, the stress results will be post-processed using Equation (1), with the value of C determined from the ultrasonic velocity and microcrack measurements. The strain results will be post-processed using Equation (5) to determine the permeability around the disposal room at specific times. The post-processing code ALGEBRA will be used. The permeability distribution around the disposal room will be overlapped with the revised DRZ. Plots of the permeability in the revised DRZ at specific times will be provided to the BRAGFLO analyst to modify the grid for the DRZ and the values of parameters related to the permeability.

3 Software List

The WIPP PA codes to be used for this analysis are listed in Table 5. These codes will be executed on Warthog. Commercial off-the-shelf (COTS) software, such as MATHEMATICA®, MATLAB®, MathCAD®, Excel®, Visio®, CorelDRAW®, Corel Paint Shop Pro X®, or Origin®, running on MS Windows XP®-based PC workstations may also be utilized. The use of any COTS application for routine calculations will be justified per NP 9-1, Appendix C and NP 19-1 as appropriate.

Table 5. Codes to be used for the revised DRZ Analysis.

Code	Version	Use
APREPRO*	1.78	Preprocessor
FASTQ*	3.12	Mesh generation
SANTOS**	2.1.7	FEM solver
ALGEBRA2*	1.22	Postprocessor
BLOT II-2*	1.39	Postprocessor

* - To be qualified per NP 19-1

** - Qualified

4 Tasks

The following tasks will be completed as part of this AP.

1. A mesh will be generated for the Room Q access drift and the structural analysis will be conducted using SANTOS.
2. The MATLAB software routines used for Holcomb and Hardy (2001) work will be verified.
3. Using ultrasonic velocity and microcrack data and results from the structural analysis, determine the best fit value for the parameter C in the damage factor criterion (Equation 1).
4. The extent of the DRZ around the disposal rooms will be determined based on the stress distribution obtained from Clay Seam G analysis.
5. Using triaxial permeability data obtained by Pfeifle et al. (1998), the fitting parameter for the Peach model will be computed.
6. Using the Peach model, permeability contours will be obtained for the DRZ using the strain distribution obtained from Clay Seam G analysis.
7. Overlapping the revised DRZ with the permeability contours, the DRZ changes with the permeability contours at specific times will be plotted.
8. The time, at which the DRZ_1 permeability parameters will be replaced with the DRZ_2 parameters, will be determined.
9. Parameters for DRZ_2 will be determined and submitted for inclusion in the WIPP PA parameter database.
10. All files related to this analysis will be stored in the Concurrent Version System (CVS).

Byoung Yoon Park will complete steps 1, 3, 4, 6, and 7; David J. Holcomb will complete step 2; Ahmed E. Ismail will complete steps 5, 8, and 9; and Thomas B. Kirchner will complete step 10. Mario J. Chavez will oversee the QA procedures. QA documentation for ultrasonic data, analysis, and documentation are planned to be completed by 30 March 2007.

5 Special Considerations

As mentioned in Section 2.3, qualification of the ultrasonic wave velocity test data must be completed before using the data in this analysis.

6 **Applicable Procedures**

All applicable WIPP QA procedures will be followed when conducting these analyses:

- Training of personnel will be conducted in accordance with the requirements of NP 2-1, *Qualification and Training*.
- Analyses will be conducted and documented in accordance with the requirements of NP 9-1, *Analyses*.
- All software used will meet the requirements laid out in NP 19-1, *Software Requirements* and NP 9-1, as applicable.
- The analyses will be reviewed following NP 6-1, *Document Review Process*.
- All required records will be submitted to the WIPP Records Center in accordance with NP 17-1, *Records*.
- New and revised parameters will be created as discussed in NP 9-2, *Parameters*.

7 **References**

- Bryan, C.R., D.W. Powers, D.M. Chapin, and F.D. Hansen, 2002. Observational studies of halite salt cores extracted from a disturbed rock zone/excavation damage zone at the Waste Isolation Pilot Plant, SAND2002-0752C, *Proposed for presentation at the North American Rock Mechanics Symposium (NARMS-TAC 2002) held July 7-10, 2002 in Toronto, Canada*.
- Butcher, B.M. 1997. *A Summary of the Sources of Input Parameter Values for the WIPP Final Porosity Surface Calculations*, SAND97-0796, Albuquerque, NM: Sandia National Laboratories.
- Carman, P. C. 1937. Fluid flow through granular beds. *Trans. Inst. Chem. Eng. London*. Vol. 15, 150-166.
- Chan, K. S., S. R. Bodner and D. E. Munson. 2001. Permeability of WIPP Salt during Damage Evolution and Healing, *Int. J. Damage Mech*. Vol. 10, 347-375.
- Chavez, M.J., 2007a. Corrective Action Request (CAR), W-07-03, dated January 5, 2007, Sandia National Laboratories.
- Chavez, M.J., 2007b. Corrective Action Plan (CAP), W-07-03, dated January 7, 2007, Sandia National Laboratories.
- Domski, P.S., D.T. Upton and R.L. Beauheim, 1996. *Hydraulic Testing around Room Q: Evaluation of the Effects of Mining on the Hydraulic Properties of Salado Evaporites*, SAND96-0435, Sandia National Laboratories, Albuquerque, NM.

- Hansen, F. D., 2003. *The Disturbed Rock Zone at the Waste Isolation Pilot Plant*. SAND2003-3407, Sandia National Laboratories, Albuquerque, NM.
- Holcomb, D. and R. Hardy, 2001. *Status of Ultrasonic Wave Speed Measurements Undertaken to Characterize the DRZ in the Assess Drift to Q Room*, Memorandum to F. Hansen, Sandia National Laboratories, dated January 22, 2001.
- Jaeger, J. C. and N. G. W. Cook, 1979. *Fundamentals of Rock Mechanics (3rd Ed)*, 84-86, Chapman and Hall, New York.
- Leigh, C. D., J. F. Kanney, L. H. Brush, J. W. Garner, R. Kirkes, T. Lowry, M. B. Nemer, J. S. Stein, E. D. Vugrin, S. Wagner, and T. B. Kirchner. 2005. *2004 Compliance Recertification Application Performance Assessment Baseline Calculation, Revision 0*. Carlsbad, NM: Sandia National Laboratories. ERMS 541521.
- Munson, D. E., A. F. Fossum and P. E. Senseny, 1989. *Advances in Resolution of Discrepancies between Predicted and Measured, In Situ Room Closures*, SAND88-2948, Albuquerque, NM: Sandia National Laboratories.
- Munson, D. E., and P. R. Dawson, 1982. *A Transient Creep Model for Salt during Stress Loading and Unloading*, SAND82-0962, Albuquerque, NM: Sandia National Laboratories.
- Park, B. Y., 2002. *Analysis Plan for the Structural Evaluation of WIPP Disposal Room raised to Clay Seam G*, AP-093, Revision 1, Sandia National Laboratories, Carlsbad, NM.
- Park, B. Y., and J. F. Holland. 2004. *Analysis Report for Structural Evaluation of WIPP Disposal Room Raised to Clay Seam G*, SAND2003-3409, Albuquerque, NM: Sandia National Laboratories.
- Park, B. Y. and J. F. Holland. 2006. *Error in DRZ Calculation in the Clay Seam G Analysis*, Memorandum to M. Y. Moo, Sandia National Laboratories, dated December 21, 2006, WIPP:1.4.1.2:PUB:QA-L:PKG#531531.
- Peach, C. J. 1991. *Influence of Deformation on the Fluid Transport Properties of Salt Rocks*, Ph.D. Thesis, Department of Geology, University of Utrecht, Netherlands.
- Pfeifle, T. W., N. S. Brodsky, and D. E. Munson. 1998. Experimental determination of the relationship between permeability and microfracture-induced damage in bedded salt. SAND98-0411C. *Proposed for presentation at the 3rd North American Rock Mechanics Symposium held June 3-5, 1998 in Cancun, Mexico*, 10 p.
- Powers, D. W., 2000. Task 2, contract 5987 (WIPP Underground Test Site Selection and Description), Memorandum to J.S. Rath, Sandia National Laboratories, dated March 31, 2000.
- Stone, C. M., 1997a. *Final Disposal Room Structural Response Calculations*, SAND97-0795, Sandia National Laboratories, Albuquerque, NM.

Stone, C.M., 1997b. *SANTOS-A Two-Dimensional Finite Element Program for the Quasistatic, Large Deformation, Inelastic Response of Solids*, SAND90-0543, Sandia National Laboratories, Albuquerque, NM.

Stormont, J. C., 1990. *Gas Permeability Changes in Rock Salt during Deformation*, Ph.D. Thesis, University of Arizona, Tucson AZ.

WIPP PA (Performance Assessment), 2003. *Verification and Validation Plan/Validation Document for SANTOS 2.1.7.* , Carlsbad, NM: Sandia National Laboratories, Sandia WIPP Central Files ERMS # 530091.

WTS (Washington TRU Solutions), 1994. S90 As-built Survey September 1993 & September 1994, Mine Engineering Departments.

NOTICE: This document was prepared as an account of work sponsored by an agency of the United States Government. Neither the United States Government nor any agency thereof, nor any of their employees, nor any of their contractors, subcontractors, or their employees, makes any warranty, express or implied, or assumes any legal liability or responsibility for the accuracy, completeness, or usefulness or any information, apparatus, product or process disclosed, or represents that its use would not infringe privately owned rights. Reference herein to any specific commercial product, process or service by trade name, trademark, manufacturer, or otherwise, does not necessarily constitute or imply its endorsement, recommendation, or favoring by the United States Government, any agency thereof or any of their contractors or subcontractors. The views and opinions expressed herein do not necessarily state or reflect those of the United States Government, any agency thereof or any of their contractors.

This document was authored by Sandia Corporation under Contract No. DE-AC04-94AL85000 with the United States Department of Energy's National Nuclear Security Administration. Parties are allowed to download copies at no cost for internal use within your organization only provided that any copies made are true and accurate. Copies must include a statement acknowledging Sandia Corporation's authorship of the subject matter.